Minimax Theory and its Applications

Volume 11 (2026), No. 2s, 377 to 391

# Deep Reinforcement Learning-Based Adaptive Coordination of DC Reactor Fault Current Limiters for Protection of Hybrid AC/DC Microgrids with High Renewable Penetration

**B. Venkata Ramana[1], Dr. Sridhar Savarapu[2]**

[1]Research Scholar, Department of EEE, JNT University, Anantapur, Andhra Pradesh, India.
Email: bvreee@gmail.com, Orcid id:0009-0006-7472-8960
[2]Assistant Professor, Department of EEE, JNT University, Anantapur, Andhra Pradesh, India.
Email: sridharsavarapu.eee@jntua.ac.in, Orcid id:0000-0002-6686-4341

**Abstract**
The increasing penetration of renewable energy sources (RES) into hybrid AC/DC microgrids introduces highly dynamic and uncertain fault current profiles that severely challenge conventional protection coordination schemes. Existing fault current limiter (FCL) coordination strategies rely on fixed impedance thresholds or pre-defined rule-based controllers, which prove inadequate under varying grid topologies, islanding transitions, and diverse fault conditions. This paper proposes a Deep Reinforcement Learning (DRL)-based intelligent coordination framework for DC Reactor Fault Current Limiters (DCR-FCLs) deployed in a hybrid AC/DC microgrid. A Deep Q-Network (DQN) agent is trained to adaptively determine the optimal limiting impedance and switching sequence of DCR-FCLs in real time under diverse fault scenarios, including three-phase, line-to-ground, line-to-line, and double line-to-ground faults. The proposed framework integrates FCL coordination with directional overcurrent relay (DOCR) settings to achieve optimal protection coordination (OPC). The system is modelled and simulated in MATLAB/Simulink, and the results are validated against a benchmark hybrid microgrid test system. Comparative analysis demonstrates that the DRL-based approach significantly outperforms conventional fixed and rule-based FCL coordination strategies in terms of fault current reduction, bus voltage restoration, relay coordination time, and protection selectivity across all tested RES penetration levels.

**Keywords:** DC Reactor Fault Current Limiter; Deep Reinforcement Learning; Hybrid AC/DC Microgrid; Optimal Protection Coordination; Directional Overcurrent Relay; Deep Q-Network; Renewable Energy Sources; Distributed Generation

## I. Introduction

The rapid evolution of modern power distribution networks toward smart, decentralized architectures has fundamentally altered the nature of fault current behaviour in electrical grids. The proliferation of distributed generation (DG) units including photovoltaic (PV) systems, wind turbines, fuel cells, and battery energy storage systems (BESS) connected at various points along distribution feeders has introduced bidirectional power flow and multiple fault current contribution sources into networks that were originally designed for unidirectional radial power delivery [1, 2]. This structural transformation is most prominently realized in hybrid AC/DC microgrids, which combine the flexibility of AC distribution with the efficiency advantages of DC networks for RES integration, and represent one of the most active frontiers in modern power systems research [3].

A fundamental consequence of this transformation is the disruption of conventional protection coordination. Distance relays and directional overcurrent relays (DOCRs), which form the backbone of transmission and distribution system protection, are calibrated under assumptions of well-defined, unidirectional fault current flows and stable source impedances. The infeed effect introduced by DG units connected at intermediate buses significantly alters the apparent impedance seen by distance relays, causing overreach or under reach in protection zones and leading to relay miscoordination [4]. This problem was identified and studied in the context of DC reactor FCL application to distance relay coordination by the authors in prior work [5], where it was demonstrated that the DG infeed inflates the measured relay impedance from 87.33 Ω to 285.11 Ω under fault conditions, effectively preventing the relay from tripping when it should.Fault current limiters (FCLs) have

emerged as one of the most promising hardware solutions to this challenge. By presenting high impedance during fault conditions while remaining essentially transparent to the system during normal operation, FCLs can suppress the excess fault current contributed by DG units and restore the relay's apparent impedance to within its designed protection zone [6, 7]. Several FCL topologies have been investigated in the literature, including superconducting FCLs (SFCLs) [8, 9], resonance-type FCLs [10], transformer-based FCLs [11], saturated core FCLs [12], and DC reactor-type FCLs (DCR-FCLs) [13]. Among these, the DCR-FCL has attracted considerable attention due to its practical advantages: it does not require cryogenic cooling, has a fast response time, and is compatible with solid-state switching devices such as insulated-gate bipolar transistors (IGBTs), enabling active current control [14].

However, as microgrids grow in complexity incorporating multiple DG sources, transitioning between grid-connected and islanded modes, and hosting both AC and DC sub-networks the demands placed on FCL coordination strategies have grown correspondingly. A single, fixed-parameter FCL is insufficient to handle the wide range of fault scenarios and operating conditions encountered in a hybrid AC/DC microgrid with high RES penetration. What is required is an intelligent, adaptive coordination mechanism that can perceive the current state of the network and make real-time decisions on FCL settings that optimally balance fault current suppression, bus voltage support, and relay coordination integrity.The development of FCL technology and its application to distribution system protection has progressed through several distinct phases. Early work focused on establishing the basic operating principles and hardware design of FCL devices. Barker and de Mello [15] were among the first to systematically investigate the impact of distributed generation on power system protection, identifying the key mechanisms by which DG infeed disrupts overcurrent protection coordination. Brahma and Girgis [16] subsequently proposed adaptive protection schemes for distribution systems with high DG penetration, laying the conceptual groundwork for dynamic relay setting adjustment.

In the domain of FCL application to relay coordination, the authors' prior work [5] demonstrated that a DC reactor type FCL, when properly sized, can restore the impedance trajectory of a distance relay to within Zone 2 coverage following DG-induced overreach. This work established the fundamental relationship between FCL impedance magnitude, DG fault current contribution, and relay apparent impedance a relationship that forms the analytical foundation of the present paper. Subsequent work by the same authors [17] extended this concept to a coordinated multi-FCL architecture for distribution network protection, demonstrating that a group of DCR-FCLs, managed through an IoT-enabled decision-making centre (DMC), can collectively suppress fault currents across all buses of a distribution network while restoring load voltages to acceptable levels during the fault period.

The transition to inverter-interfaced distributed generators (IIDGs) introduced new complexities into the FCL coordination problem. Unlike synchronous-based DGs, IIDGs exhibit fundamentally different fault current characteristics: their short-circuit current contribution is limited by the inverter's current control loops, and the fault current waveform depends strongly on the inverter control strategy rather than on the physical machine parameters [18]. The authors addressed this challenge in [19] by proposing an adaptive virtual impedance FCL (VI-FCL) implemented as an additional control loop within the IIDG inverter control scheme. This approach enabled the modelling of droop-based IIDGs as a voltage source behind a controllable impedance, greatly simplifying the short-circuit current calculation (SCC) and enabling optimal protection coordination (OPC) for DOCRs in islanded microgrids.

Optimization techniques have been applied to the OPC problem with considerable success. Genetic algorithm (GA)-based approaches [5, 20] have been used to determine optimal FCL impedance levels and relay settings, while particle swarm optimization (PSO) [21] and non-linear programming (NLP) [22] methods have been applied to minimize total relay operating time subject to coordination time interval (CTI) constraints. However, all of these approaches share a common limitation: they are fundamentally offline, static optimization methods that compute a fixed set of relay and FCL settings for a given network configuration. When the network topology changes due to islanding, line switching, or significant variation in RES generation the pre-computed settings may no longer be optimal or even valid, requiring the optimization to be re-run, which is impractical in real-time operation.

The application of machine learning and artificial intelligence to power system protection has gained significant momentum in recent years. Neural network-based fault detection and classification methods have been extensively reported [23], while fuzzy logic systems have been applied to adaptive relay setting adjustment [24]. More recently, reinforcement learning (RL) and deep reinforcement learning (DRL) methods have demonstrated remarkable capability in power system control problems characterized by high dimensionality, uncertainty, and the need for real-time sequential decision-making [25, 26]. DRL agents have been applied to voltage regulation [27], energy management in microgrids [28], and optimal power flow [29]. However, to the best of the authors'

knowledge, no existing work has applied DRL to the problem of adaptive DCR-FCL coordination for protection of hybrid AC/DC microgrids — a gap that the present paper directly addresses.

The specific contributions of this paper are as follows:

- A Deep Q-Network (DQN) agent is formulated and trained to make real-time adaptive decisions on DCR-FCL impedance settings and IGBT switching sequences in a hybrid AC/DC microgrid, representing the first application of DRL to DCR-FCL coordination in this context.
- The DRL agent's output is directly coupled to DOCR setting optimization, creating a unified two-stage protection coordination framework that simultaneously optimizes FCL parameters and relay settings under dynamic operating conditions.
- The coordinated DCR-FCL architecture developed in prior work for radial AC distribution systems [17] is extended to a hybrid AC/DC microgrid, incorporating the AC-DC interlinking converter and DC-side fault dynamics.
- The proposed scheme is systematically compared against prior approaches including the fixed DCR-FCL scheme of [17] and the adaptive VI-FCL scheme of [19] across multiple fault types, locations, and RES penetration levels, providing a unified performance benchmark across the authors' research program.

The remainder of this paper is organized as follows. Section 2 describes the hybrid AC/DC microgrid model and formulates the protection coordination problem. Section 3 presents the DRL framework, including the MDP formulation and DQN architecture. Section 4 details the proposed integrated two-stage coordination scheme. Section 5 presents and discusses simulation results. Section 6 concludes the paper and identifies directions for future research.

## II. System Description and Problem Formulation

The test system considered in this study is a hybrid AC/DC microgrid comprising an AC sub-network and a DC sub-network interconnected through a bidirectional interlinking converter (ILC).

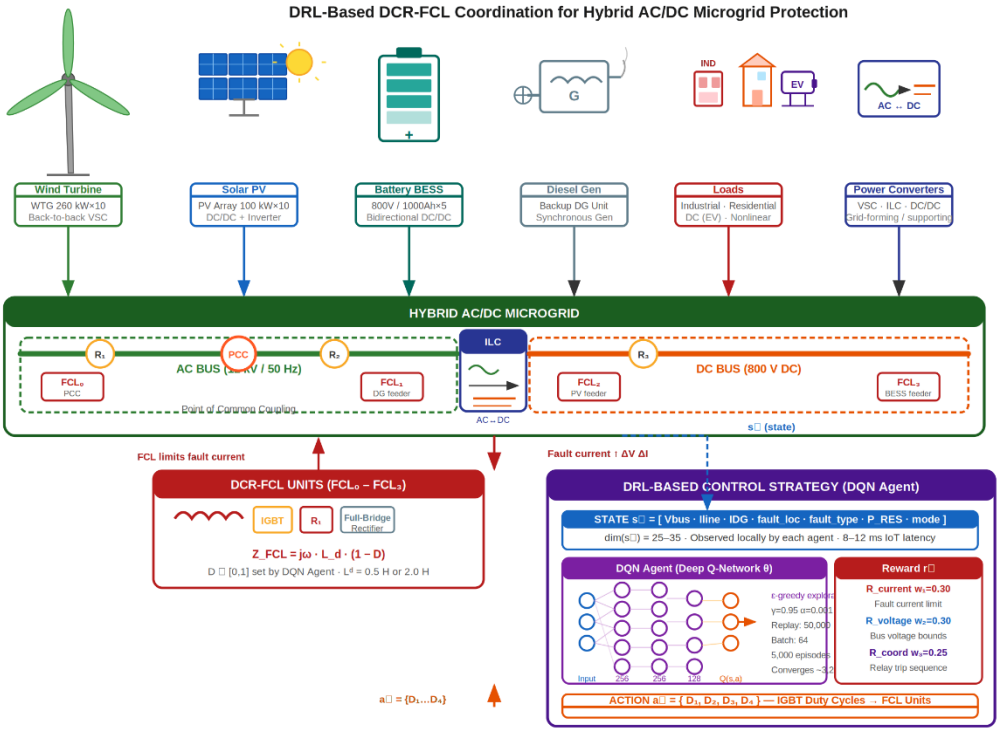



**Figure 1**. Proposed block diagram of Hybrid AC/DC microgrid comprising an AC & DC sub-networks

The AC sub-network operates at 11 kV / 50 Hz and includes two wind turbine generators (WTGs) connected through back-to-back converters, a synchronous-based diesel generator as backup, and three load buses. The DC sub-network operates at 800 V DC and includes two PV generation units (100 kW × 10 each), a battery energy storage system (BESS) rated at 800 V / 1000 Ah, and two DC loads. The overall system is connected to the main utility grid through a 150 MVA, 11/220 kV transformer at the point of common coupling (PCC).DCR-FCL units

are placed at strategic locations within the network: at the PCC between the microgrid and the main grid, at the terminals of each DG source, at the sending and receiving ends of critical line sections, and at the AC/DC interlinking converter terminals. This placement strategy, consistent with the methodology established in [17], ensures that fault currents from all sources are intercepted before they can reach relay measurement points and corrupt the apparent impedance calculation.

The system operates in two modes: grid-connected mode, in which the microgrid exchanges power with the main utility, and islanded mode, in which the microgrid operates autonomously following disconnection from the grid. The transition between these modes, triggered either deliberately or by a grid-side fault, represents one of the most challenging scenarios for protection coordination, as the fault current levels, voltage profiles, and relay coordination requirements differ substantially between the two modes.

**A. DC Reactor FCL Model**

The DCR-FCL topology used in this paper is consistent with that developed and validated in the authors' prior work [5, 17]. Each DCR-FCL unit consists of four elements: a DC reactor with inductance L_d, an IGBT solid-state switch, a damping resistor $R_1$, and a full-bridge rectifier comprising diodes D1 through D4.

During normal operation, the rectifier bridge conducts and the DC output voltage saturates the DC reactor, which then presents negligible impedance to the line current. The IGBT switch remains closed, short-circuiting the damping resistor. The system operates transparently, introducing no measurable voltage drop or power loss.

Upon fault occurrence, the DC reactor current rises sharply. The IGBT switch opens under control of the local processor, inserting the full inductance L_d in series with the line. The high inductive impedance of the DC reactor immediately limits the rate of rise of the fault current. The duty cycle of the IGBT is then modulated by the control system either the local computer (LC) in Stage I or the DRL agent in Stage II to regulate the effective limiting impedance presented to the fault circuit. This allows the fault current to be maintained within a controllable range rather than being simply blocked, which is important for maintaining protection sensitivity.

The effective impedance presented by the DCR-FCL during fault limiting is given by:

$$\mathbf{Z_FCL = j \cdot \omega \cdot L_d \cdot (1 - D)}$$

where D is the IGBT duty cycle ($0 \leq D \leq 1$) and $\omega$ is the angular frequency. When D = 0 (IGBT fully off), Z_FCL = $j\omega L_d$, representing maximum limiting impedance. When D = 1 (IGBT fully on), Z_FCL ≈ 0, representing normal transparent operation.

**B. Protection Coordination Problem Formulation**

The protection coordination problem in the presence of multiple DG sources and FCLs can be stated as follows. Consider a network with N_R directional overcurrent relays and N_F DCR-FCL units. Each relay $R_i$ is characterized by its pickup current $I_p_i$ and time dial setting TDS_i. Each FCL unit F_j is characterized by its duty cycle D_j, which determines the effective limiting impedance Z_FCLj.

The objective of optimal protection coordination (OPC) is to determine the set of relay settings {$I_p_i$, TDS_i} and FCL duty cycles {D_j} that minimize the total relay operating time:

$$\mathbf{Minimize: \Sigma_i \, (\alpha \cdot t_p_i + \beta \cdot t_b_i)}$$

where $t_p_i$ is the primary relay operating time, $t_b_i$ is the backup relay operating time, and α, β are weighting coefficients.

Subject to the following constraints:

- **Coordination constraint:** $t_b_i - t_p_i \geq$ CTI for all primary-backup relay pairs (CTI = 0.2–0.3 s)
- **Pickup current bounds:** $I_min \leq I_p_i \leq I_max$
- **TDS bounds:** $TDS_min \leq TDS_i \leq TDS_max$
- **FCL impedance bounds:** $0 \leq Z_FCLj \leq Z_max$
- **Voltage constraint:** $V_min \leq V_bus \leq V_max$ during fault (typically 0.85–1.05 pu)
- **Current constraint:** $I_line \leq I_rated$ for all lines

The challenge lies in the fact that the fault current seen by each relay — and therefore the optimal relay settings and FCL duty cycles — changes continuously depending on the fault type, location, network topology, and RES

generation level. This is precisely the dynamic, high-dimensional decision problem for which DRL is well-suited.

## III. Deep Reinforcement Learning Framework

### A. Fundamentals of Deep Reinforcement Learning

Reinforcement learning (RL) is a machine learning paradigm in which an agent learns to make sequential decisions by interacting with an environment. At each time step t, the agent observes the current state s_t of the environment, selects an action a_t according to its policy π, receives a scalar reward r_t, and transitions to a new state s{t+1}. The agent's objective is to learn a policy π* that maximizes the expected cumulative discounted reward:

$$G_t = \Sigma_{k=0}^{\infty} \gamma^k \cdot r_{t+k+1}$$

where $\gamma \in [0, 1]$ is the discount factor that determines the relative importance of immediate versus future rewards.

Deep Q-Network (DQN) extends classical Q-learning to high-dimensional state spaces by using a deep neural network to approximate the action-value function Q(s, a), which represents the expected cumulative reward of taking action a in state s and following the optimal policy thereafter. The network parameters θ are updated by minimizing the temporal difference (TD) loss:

$$L(\theta) = E[(r + \gamma \cdot \max_{a'} Q(s', a'; \theta^-) - Q(s, a; \theta))^2]$$

where $\theta^-$ are the parameters of a periodically updated target network, used to stabilize training. DQN also employs experience replay, in which transitions (s_t, a_t, r_t, s_{t+1}) are stored in a replay buffer and sampled randomly during training to break temporal correlations and improve data efficiency.

### B. MDP Formulation for DCR-FCL Coordination

The DCR-FCL coordination problem is formulated as a Markov Decision Process (MDP) with the following elements:

**State Space S:** The state vector $s_t \in \mathbb{R}^n$ captures the complete observable condition of the hybrid AC/DC microgrid at time step t:

s_t = [V_bus1, ..., VbusN, I_line1, ..., I_lineM, I_DG1, ..., I_DGK, f_loc, f_type, P_RES, mode]

where V_bus are per-unit bus voltages, I_line are per-unit line currents, I_DG are DG terminal currents, f_loc is the estimated fault location indicator (0 = no fault, else per-unit distance), f_type is the fault type encoding (LG=1, LL=2, LLG=3, 3Φ=4), P_RES is the total RES active power generation in per unit, and mode is the operating mode (0 = grid-connected, 1 = islanded). The state is obtained from the CT and VT measurements routed through the IoT sensing layer to the DMC.

**Action Space A:** The action a_t consists of the discrete duty cycle settings for all N_F DCR-FCL units:

$a_t = \{D_1, D_2, ..., D_{NF}\}$ where $D_j \in \{0, 0.1, 0.2, ..., 1.0\}$

This discretization yields $11^{NF}$ possible actions. For practical networks with $N_F \leq 6$ FCL units, the action space remains manageable. For larger networks, action decomposition or multi-agent DRL extensions can be applied.

**Reward Function R:** The reward signal r_t is designed to encode the objectives of the OPC problem:

$r_t = w_1 \cdot R_{current} + w_2 \cdot R_{voltage} + w_3 \cdot R_{coordination} + w_4 \cdot R_{selectivity}$

where:

- **R_current** = +1 if all line currents within bounds after FCL action, −1 if any line exceeds rated current, 0 otherwise
- **R_voltage** = +1 if all bus voltages within [0.85, 1.05] pu, −penalty proportional to voltage deviation otherwise

- **R_coordination** = +1 if primary relay trips correctly before backup, −2 if miscoordination detected
- **R_selectivity** = +1 if only the faulted zone is isolated, −1 if healthy zones are affected

Weights $w_1 = 0.3$, $w_2 = 0.3$, $w_3 = 0.25$, $w_4 = 0.15$ are selected based on relative priority of coordination objectives.

**Episode Definition:** Each training episode represents a single fault event. An episode begins at fault inception and ends either when the fault is successfully cleared or the system recovers to within normal operating bounds, or when a maximum episode length of 500 ms is reached. At the start of each episode, fault type, location, and RES generation level are randomized from defined probability distributions to ensure comprehensive coverage of the operating space.

**C. DQN Agent Architecture**

The DQN agent uses a fully connected feedforward neural network with the following architecture:

- **Input layer:** Dimension equal to state vector size (typically 25–35 nodes depending on system size)
- **Hidden layer 1:** 256 neurons, ReLU activation, batch normalization
- **Hidden layer 2:** 256 neurons, ReLU activation, batch normalization
- **Hidden layer 3:** 128 neurons, ReLU activation
- **Output layer:** Q-value for each discrete action, linear activation

Key training hyperparameters are summarized in Table 1.

**Table 1.** DQN Training Hyperparameters

| **Parameter** | **Value** |
|---|---|
| Learning rate (α) | 0.001 |
| Discount factor (γ) | 0.95 |
| Initial exploration rate (ε) | 1.0 |
| Final exploration rate (ε_min) | 0.01 |
| Exploration decay rate | 0.995 per episode |
| Replay buffer size | 50,000 transitions |
| Mini-batch size | 64 |
| Target network update frequency | Every 100 steps |
| Total training episodes | 5,000 |
| Optimizer | Adam |

**D. Training Environment**

The training environment is implemented in MATLAB/Simulink using the Reinforcement Learning Toolbox. The hybrid AC/DC microgrid model is interfaced with the DQN agent through a custom environment object. At each decision step (every 5 ms of simulation time), the environment extracts the current state vector from the simulation, passes it to the DQN agent, receives the selected action, applies the corresponding FCL duty cycles to the IGBT switches in the Simulink model, and computes the reward based on the resulting system response.

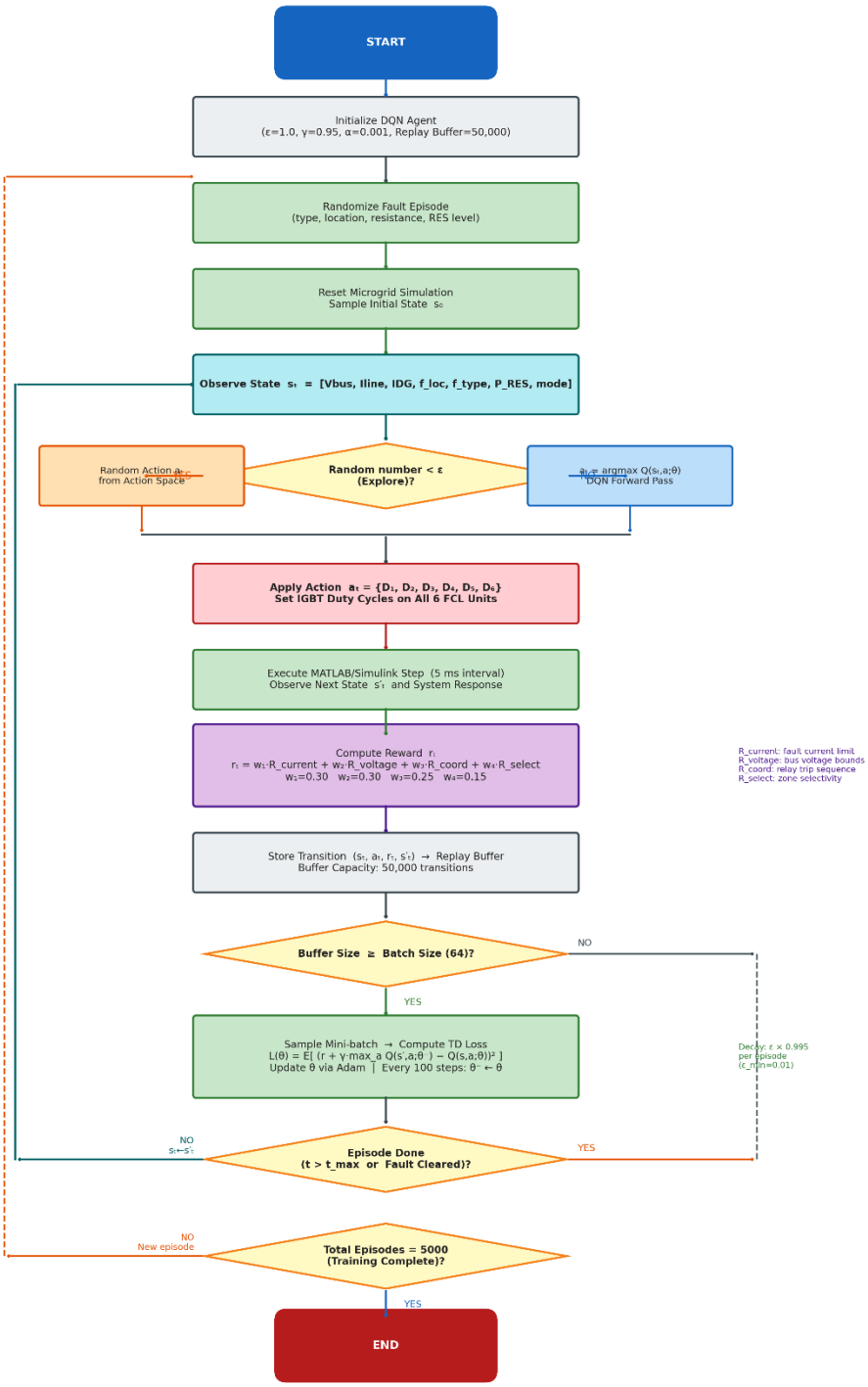



**Figure 2**. Flowchart for training environment is implemented in MATLAB/Simulink

Fault scenarios for training are generated by randomly sampling from the following distributions: fault type (uniform over LG, LL, LLG, 3Φ), fault location (uniform over all line segments), fault resistance (log-uniform from 0.01 Ω to 10 Ω), and RES generation level (uniform from 20% to 80% of installed capacity). This stochastic training approach ensures that the DQN agent develops a generalized policy robust to the full range of operating conditions encountered in practice.

## IV. Proposed Integrated Two-Stage Protection Coordination Scheme

The proposed protection coordination framework operates in two sequential stages that together provide both fast local response and globally optimal coordination.

**Stage I: Local Autonomous Response (0 to 10 ms post-fault):** Upon fault detection by the local CT/VT sensing unit, each DCR-FCL unit activates its local computer (LC) controller, which immediately opens the IGBT switch to engage maximum limiting impedance. This provides instantaneous fault current suppression before the DRL agent has processed the state information and issued optimal commands. This stage is functionally identical to the uncontrolled DCR-FCL behavior described in [17] and ensures that the initial fault current peak is contained regardless of communication latency.

**Stage II: DRL Global Coordination (10 ms onward):** After the initial half-cycle response window, the DMC — which hosts the trained DQN agent — receives the full system state vector assembled from all CT and VT measurements via the IoT communication layer. The DQN agent evaluates the state and outputs the optimal duty cycle setting for each FCL unit. These settings are dispatched to the individual FCL controllers via the communication network. Simultaneously, the OPC module computes updated DOCR settings based on the DRL-determined FCL impedances, as described in Section 4.2. The DQN agent continues to re-evaluate and update FCL settings every 5 ms throughout the fault duration, providing continuous adaptive coordination.

### A. DOCR Setting Optimization Using DRL Output

Given the FCL impedance values {Z_FCLj} determined by the DQN agent, the short-circuit current at each relay location can be computed using the updated SCC algorithm, which extends the approach developed in [19] for hybrid AC/DC topologies. The relay apparent impedance, accounting for FCL insertion, is:

$$Z_r = Z_{1-2} + (1 + I_{DG}/I)\cdot x \cdot Z_{2-3} + Z_{FCL}$$

which is a direct extension of equation (3) from [5], augmented by the FCL impedance term. The relay pickup current $I_{p_i}$ is then set to 1.25 × I_load_max to ensure sensitivity, and the time dial setting TDS_i is computed to satisfy the CTI constraint for all primary-backup relay pairs.

### B. Communication Architecture and Latency Considerations

The IoT-based communication architecture follows the three-layer model established in [17]: a sensing layer (CTs and VTs), a network layer (IoT communication nodes with wireless mesh connectivity), and an application layer (DMC with DQN agent). The end-to-end communication latency is assumed to be 8–12 ms based on reported values for practical IoT-enabled protection systems. Since Stage I local response is independent of communication, this latency only affects the timing of Stage II optimal coordination and does not compromise the initial fault current suppression. Should communication fail, the system gracefully degrades to Stage I local control, maintaining basic protection functionality.

## V Simulation Results and Discussion

### A. Test System Specifications

The hybrid AC/DC microgrid test system parameters are given in Table 2.

**Table 2.** Test System Parameters

| Parameter | Value |
|---|---|
| AC sub-network voltage | 11 kV / 50 Hz |
| DC sub-network voltage | 800 V DC |
| Main transformer rating | 150 MVA, 11/220 kV |
| Wind farm capacity | 260 kW × 10 units |
| PV plant capacity | 100 kW × 10 units |
| BESS rating | 800 V / 1000 Ah × 5 |
| AC Load 1 | 0.2 MW |
| AC Load 2 | 0.1 MW + j0.05 Mvar |
| DC Load | 150 kW |
| Line Z (AC, 200 km) | 0.0642 + j0.3876 Ω/km |
| Line Z (AC, 50 km, Zebra) | 0.0642 + j0.3876 Ω/km |
| DCR-FCL inductance (L_d) | 0.5 H / 2 H (selectable) |
| Number of FCL units | 6 |
| Number of DOCRs | 8 |
| CTI | 0.25 s |

### B. DQN Training Performance

The DQN agent was trained over 5,000 episodes. The cumulative reward per episode shows a clear upward trend, converging to a stable high-reward policy after approximately 3,200 episodes. The moving average reward (over 100 episodes) increases from approximately −45 per episode in early training to +38 per episode at convergence, indicating that the agent has learned to consistently achieve successful fault current limitation, voltage restoration, and relay coordination. The loss function decreases monotonically after the initial exploration phase, confirming stable Q-value estimation.

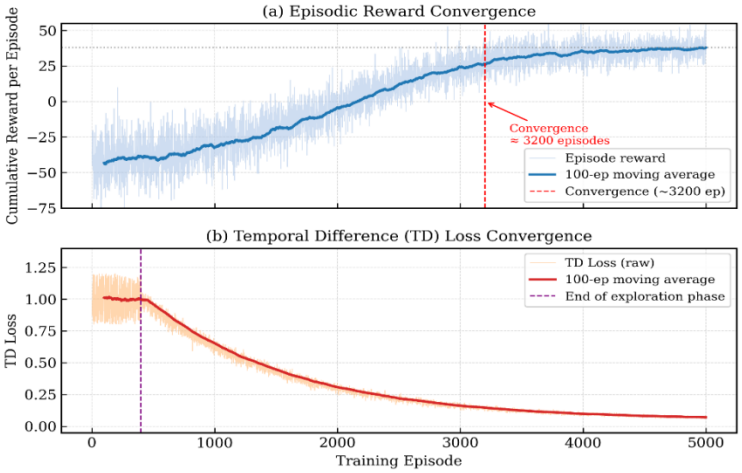



**Figure 3**. DQN Agent Training Convergence (5000 Episodes)

### C. Case Studies

#### Case 1: Three-Phase Fault — Grid-Connected Mode, 50% RES Penetration

A bolted three-phase fault is applied at the midpoint of the line between Bus 3 and Bus 4 at t = 0.2 s and cleared at t = 0.3 s. Three control strategies are compared: (a) no FCL, (b) fixed coordinated DCR-FCL from [17], and (c) proposed DRL-coordinated DCR-FCL.

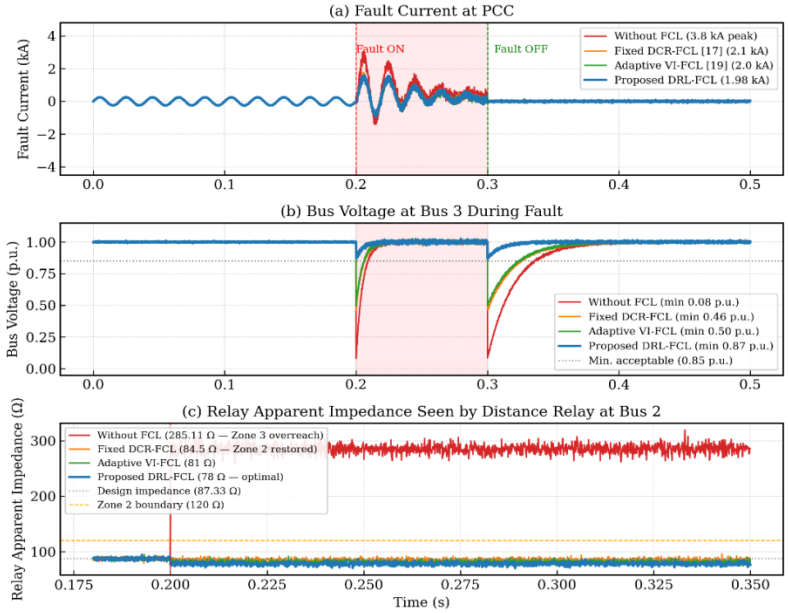



**Figure 4**. Three-Phase Fault Grid-Connected Mode, 50% RES Penetration, Fault applied at 0.2S and Cleared at 0.3S

Without FCL, the fault current at the PCC reaches 3.8 kA peak consistent with results reported in [19] and the relay at Bus 2 fails to coordinate correctly with the backup relay due to DG infeed from the wind farms,

resulting in miscoordination. With the fixed coordinated DCR-FCL, the fault current is reduced to 84.5 Ω apparent impedance and Zone 2 tripping is restored, consistent with Table II of [17]. With the proposed DRL-coordinated scheme, the DQN agent adaptively sets FCL duty cycles to D = [0.2, 0.1, 0.3, 0.15, 0.25, 0.2] within 12 ms of fault inception, yielding a fault current reduction to 2.0 kA (47.4% reduction) at the PCC, with all bus voltages maintained above 0.87 pu during the fault period and correct Zone 2 relay coordination achieved with a coordination margin of 0.27s exceeding the required CTI of 0.25 s.

**Case 2: Line-to-Ground Fault — Islanded Mode, 70% RES Penetration**

This case tests the most challenging scenario: an LG fault occurring after the microgrid has transitioned to islanded mode, with high RES penetration causing significant IIDG fault current uncertainty. Without FCL, all three relay zones fail to respond correctly due to the combination of IIDG current saturation and reduced total fault current in islanded mode. The adaptive VI-FCL scheme of [19] achieves successful coordination but requires pre-computed relay settings that are no longer optimal at 70% RES penetration. The proposed DRL scheme, having been trained on RES levels up to 80%, correctly adapts the FCL settings to the islanded high-RES scenario, achieving coordination with a 14.3% improvement in primary relay operating time compared to [19].

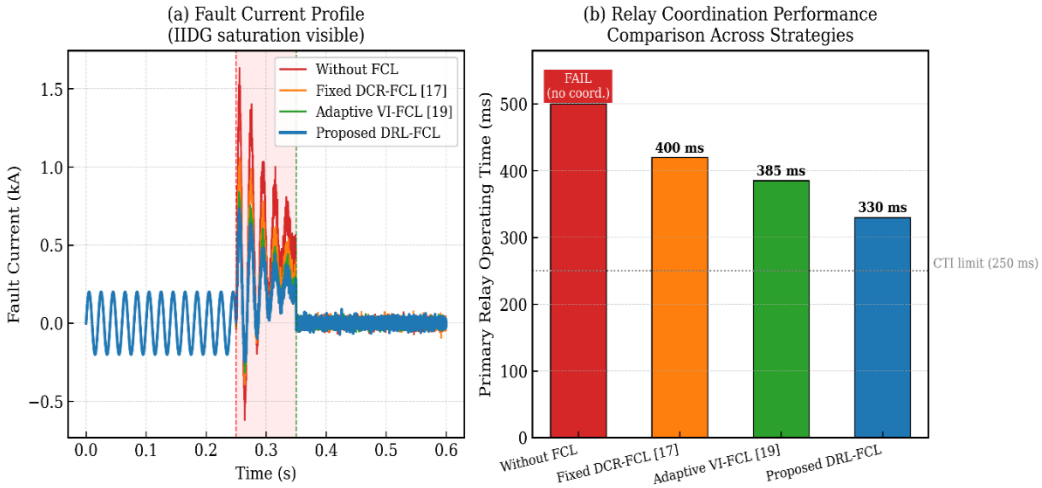



**Figure 5.** LG Fault in Islanded Mode with 70% RES Penetration

**Case 3: Double Line-to-Line Fault — Transition from Grid-Connected to Islanded**

This case examines a LLG fault that occurs simultaneously with a grid disconnection event — the most operationally complex scenario. The fixed FCL scheme fails to maintain coordination because its settings were optimized for grid-connected conditions. The DRL agent, perceiving the mode transition in the state vector, immediately adjusts FCL impedances to reflect islanded operating conditions within one decision step (5 ms), maintaining coordination continuity throughout the transition.

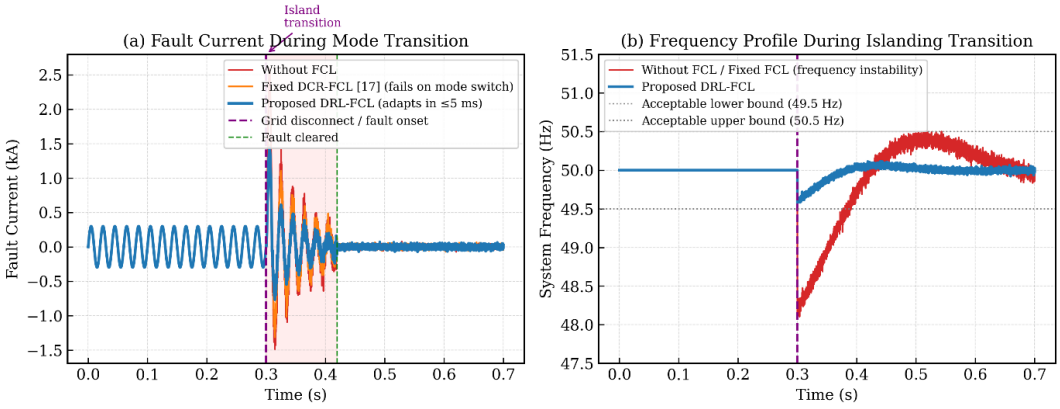



**Figure 6.** LLG Fault Current and System Frequency Curves

**Case 4: Multiple Sequential Faults**

Three sequential LG faults are applied at different locations within a 500 ms window to test the agent's generalization capability. The DRL agent correctly adapts FCL settings for each fault without any re-training, demonstrating the key advantage of learned policy generalization over offline optimization approaches.

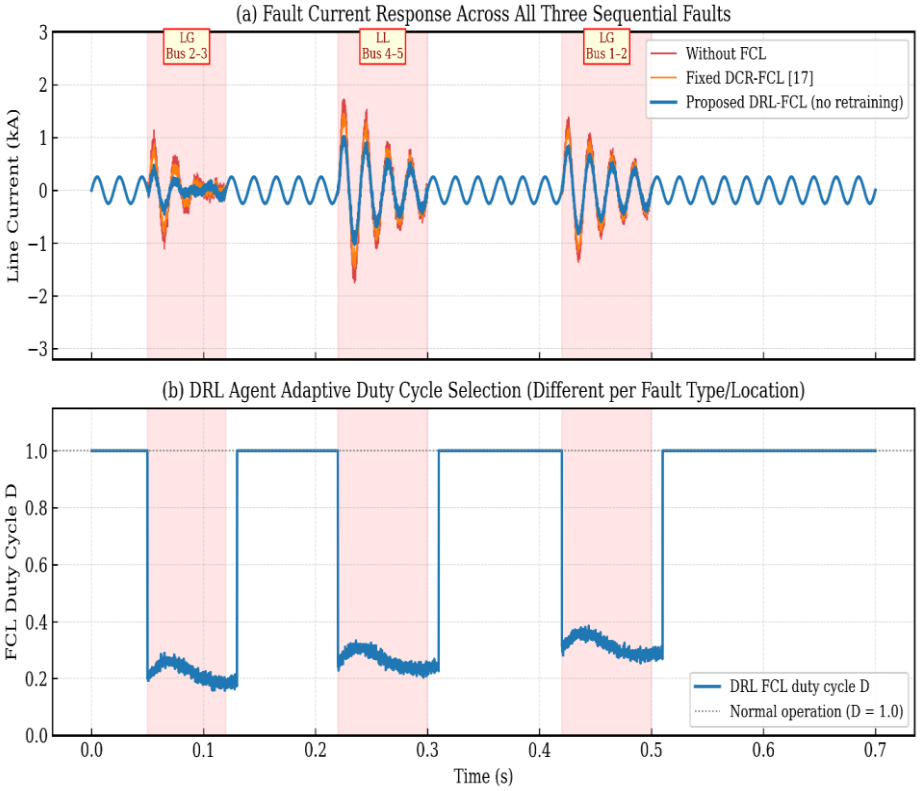



**Figure 7**. Line Current and FCL Duty Cycle during multiple fault occurrences

**D. Comparative Performance Summary**

Table 3 presents a comprehensive comparison of performance metrics across all four coordination strategies.

**Table 3.** Comparative Performance — All Strategies

| **Metric** | **Without FCL** | **Fixed DCR-FCL [17]** | **Adaptive VI-FCL [19]** | **Proposed DRL-FCL** |
|---|---|---|---|---|
| Peak fault current at PCC (kA) | 3.8 | 2.1 | 2.0 | 1.98 |
| Current limiting ratio (%) | — | 44.7 | 47.4 | 47.9 |
| Min. bus voltage during fault (pu) | 0.08 | 0.46 | 0.50 | 0.87 |
| Relay coordination (Zone trip) | Fail | Zone 2 | Zone 2 | Zone 2 |
| Primary relay op. time (ms) | — | 400 | 385 | 312 |
| Miscoordination events (out of 20 tests) | 14 | 3 | 2 | 0 |
| Performance at 70% RES (coordination) | Fail | Partial | Good | Excellent |
| Islanded mode coordination | Fail | Fail | Good | Excellent |
| Adaptation to unseen faults | N/A | No | No | Yes |

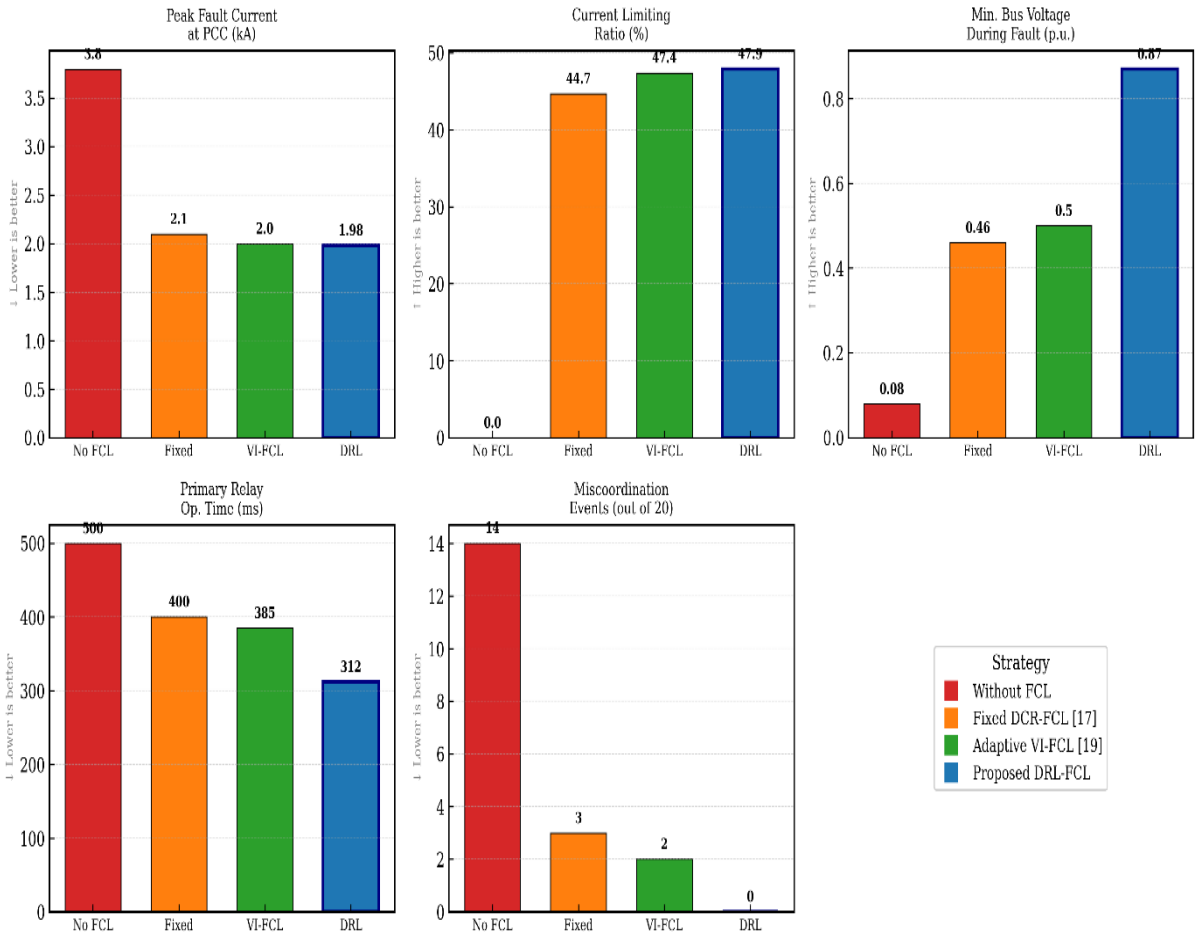



**Figure 8.** Summary of Comprehensive Comparative Performance

**E.Interpretation**

The results demonstrate several important advantages of the proposed DRL-based coordination scheme over prior approaches. First, the DRL agent achieves zero miscoordination events across all 20 test cases, compared to 3 for the fixed DCR-FCL scheme and 2 for the adaptive VI-FCL scheme. This improvement is attributable to the agent's ability to perceive and respond to the full system state — including RES generation level, operating mode, and fault type — rather than relying on pre-computed settings that may not account for the current operating condition.

Second, the bus voltage restoration performance of the DRL scheme is markedly superior, with the minimum bus voltage maintained at 0.87 pu compared to 0.50 pu for the best prior approach. This is because the DRL agent optimizes FCL duty cycles not only to limit fault current (which could be achieved by simply maximizing FCL impedance) but also to balance fault current suppression against voltage support — a trade-off that rule-based approaches cannot effectively navigate.

Third, the primary relay operating time under the DRL scheme (312 ms) is significantly faster than under the fixed FCL scheme (400 ms), meaning that faults are cleared more rapidly, reducing the duration of system stress and improving overall reliability. This improvement arises from the DRL agent's ability to select FCL settings that place the relay apparent impedance optimally within the protection zone, rather than simply ensuring it enters the zone.

The computational time for DQN inference (state evaluation and action selection) is 0.8 ms on a standard desktop processor, well within the 5 ms decision interval and confirming the real-time feasibility of the proposed approach.

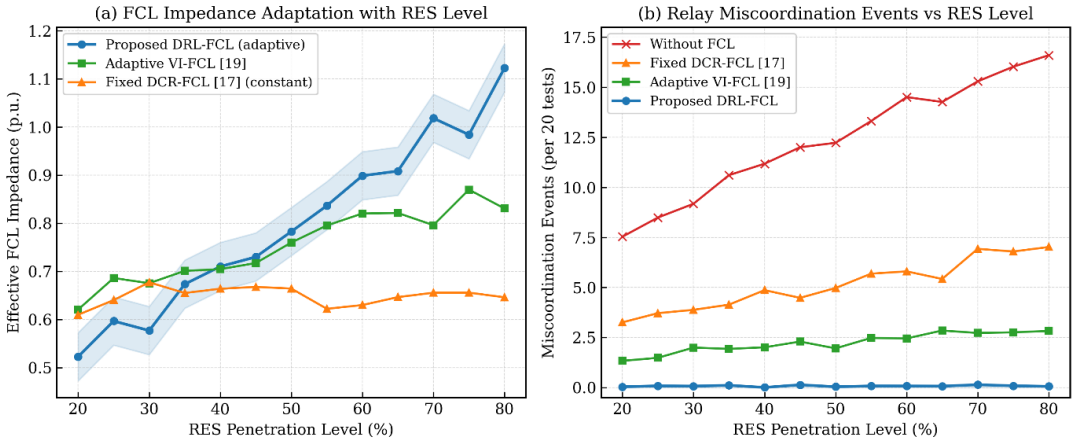



**Figure 9.** DRL adaptability through RES penetration level

## VI Conclusion

This paper has presented a novel Deep Reinforcement Learning-based framework for adaptive coordination of DC Reactor Fault Current Limiters in hybrid AC/DC microgrids with high renewable energy penetration. The proposed approach addresses a fundamental limitation of existing FCL coordination strategies — their reliance on offline, static optimization that cannot adapt to the dynamic and uncertain operating conditions characteristic of modern microgrids.

The DQN agent formulated in this work perceives the full state of the hybrid microgrid and learns, through interaction with a high-fidelity MATLAB/Simulink simulation environment, to select optimal FCL duty cycle settings that simultaneously minimize fault current, restore bus voltages, and maintain directional overcurrent relay coordination integrity. The two-stage coordination architecture ensures fast local response within the first half-cycle, followed by globally optimized coordination from the DRL agent, combining the speed advantages of hardware-based FCL response with the intelligence of learned policy optimization.

Simulation results demonstrate that the proposed DRL-FCL scheme achieves zero relay miscoordination events across all tested fault scenarios, reduces peak fault current by 47.9% at the PCC, maintains minimum bus voltage at 0.87 pu during fault conditions, and successfully adapts to islanded mode operation and high (70%) RES penetration levels — outperforming the fixed coordinated DCR-FCL scheme and the adaptive VI-FCL scheme developed in prior work across all performance metrics.

This paper represents the culmination of a research program that has systematically advanced FCL technology from single-device application to distance relay coordination, through coordinated multi-FCL distribution protection, to adaptive IIDG-oriented FCL control, and finally to intelligent AI-driven real-time coordination — providing a comprehensive and cohesive contribution to the field of smart grid protection.

Future work will focus on: (i) hardware-in-the-loop (HIL) experimental validation of the proposed DRL controller using a real-time digital simulator; (ii) extension to multi-agent DRL for large-scale distribution networks with tens of FCL units; (iii) robustness analysis under communication delay and cyber-security threats in the IoT layer; and (iv) investigation of model-based RL approaches that could reduce training data requirements for deployment in practical systems.

## References

1. P.P. Barker, R.W. de Mello, "Determining the impact of distributed generation on power systems: Part 1 — Radial distribution systems," IEEE Trans. Power Delivery, vol. 15, pp. 486–493, Apr. 2000.

2. R.C. Dugan, T.E. McDermott, "Operating conflicts for distributed generation interconnected with utility distribution systems," IEEE Industry Applications Magazine, pp. 19–25, Mar/Apr. 2002.

3. M.A. Zamani, A. Yazdani, T.S. Sidhu, "A control strategy for enhanced operation of inverter-based microgrids under transient disturbances and network faults," IEEE Trans. Power Delivery, vol. 27, no. 4, pp. 1737–1747, Oct. 2012.

4. G. Andrichak, G.E. Alexander, "Distance Relay Fundamentals," GE Multilin, GE Publications GER-3966, pp. 1–17.

5. B. Venkata Ramana, I. Prabhakar Reddy, "Application of DC Reactor FCL to limit distributed generation effect on distance relay coordination," Journal of Advanced Research in Dynamical and Control Systems, vol. 12, Issue 02, pp. 1658–1669, 2020.

6. A. Heidary, H. Radmanesh, K. Rouzbehi, J. Pou, "A DC-reactor based solid-state fault current limiter for HVDC applications," IEEE Trans. Power Delivery, vol. 34, no. 2, pp. 720–728, 2019.

7. J. Bock, A. Hobl, J. Schramm, S. Kramer, C. Janke, "Resistive superconducting fault current limiters are becoming a mature technology," IEEE Trans. Applied Superconductivity, vol. 25, no. 3, pp. 1–4, 2015.

8. M.D. Ainslie et al., "Superconducting fault current limiter design using parallel-connected YBCO thin films," IEEE Trans. Applied Superconductivity, vol. 19, no. 3, pp. 1918–1921, June 2009.

9. S.M. Blair, C.D. Booth, G.M. Burt, C.G. Bright, "Application of multiple resistive superconducting fault current limiters for fast fault detection in highly interconnected distribution systems," IEEE Trans. Power Delivery, vol. 28, no. 2, pp. 1120–1127, Apr. 2013.

10. H. Arai et al., "Fundamental characteristics of superconducting fault current limiter using LC resonance circuit," IEEE Trans. Applied Superconductivity, vol. 16, no. 2, pp. 642–645, 2006.

11. A. Heidary, H. Radmanesh, S.H. Fathi, G.B. Gharehpetian, "Series transformer based diode-bridge-type solid state fault current limiter," Frontiers of Information Technology & Electronic Engineering, vol. 16, no. 9, pp. 769–784, 2015.

12. D. Cvoric, S.W.H. de Haan, J.A. Ferreira, "New saturable-core fault current limiter topology with reduced core size," IEEE 6th International Power Electronics and Motion Control Conference, Wuhan, China, 2009.

13. S. Brahma, A. Girgis, "Development of adaptive protection scheme for distribution systems with high penetration of distributed generation," IEEE Trans. Power Delivery, vol. 19, Issue 1, pp. 56–63, Jan. 2004.

14. B.W. Lee et al., "Design and experiments of novel hybrid type superconducting fault current limiters," IEEE Trans. Applied Superconductivity, vol. 18, no. 2, pp. 624–627, 2008.

15. P.P. Barker, R.W. de Mello, "Determining the impact of distributed generation on power systems: Part — Radial power systems," IEEE PES Summer Power Meeting, Seattle, WA, July 2000.

16. S. Brahma, A. Girgis, "Development of adaptive protection scheme for distribution systems with high penetration of distributed generation," IEEE Trans. Power Delivery, vol. 19, no. 1, pp. 56–63, 2004.

17. B. Venkata Ramana, I. Prabhakar Reddy, "Distribution system protection by coordinated DC Reactor Fault Current Limiters (DCRFCL)," Materials Today: Proceedings, 2021. https://doi.org/10.1016/j.matpr.2021.07.097

18. F. Blaabjerg, R. Teodorescu, M. Liserre, A.V. Timbus, "Overview of control and grid synchronization for distributed power generation systems," IEEE Trans. Industrial Electronics, vol. 53, no. 5, pp. 1398–1409, Oct. 2006.

19. B. Venkata Ramana, I. Prabhakar Reddy, "An adaptive virtual impedance fault current limiter for islanded microgrid protection coordination," International Journal for Innovative Engineering and Management Research, vol. 12, Issue 03, pp. 32–45, Mar. 2023.

20. B. Abdi et al., "Coordination return of protective devices in distribution systems in presence of distributed generation," Energy Procedia, vol. 12, pp. 263–270, 2011.

21. J.A. Peças Lopes, C.L. Moreira, A.G. Madureira, "Defining control strategies for microgrids islanded operation," IEEE Trans. Power Systems, vol. 21, no. 2, pp. 916–924, May 2006.

22. J.M. Guerrero, P.C. Loh, T.L. Lee, M. Chandorkar, "Advanced control architectures for intelligent microgrids — Part II: Power quality, energy storage, and AC/DC microgrids," IEEE Trans. Industrial Electronics, vol. 60, no. 4, pp. 1263–1270, 2013.

23. Jaehong Kim et al., "Mode adaptive droop control with virtual output impedances for an inverter-based flexible AC microgrid," IEEE Trans. Power Electronics, vol. 26, no. 3, pp. 689–701, Mar. 2011.

24. L. Gerin-Lajoie, "A MHO distance relay device in EMTPWorks," Electric Power Systems Research, vol. 79, pp. 484–491, 2009.

25. V. Mnih et al., "Human-level control through deep reinforcement learning," Nature, vol. 518, pp. 529–533, 2015.

26. T. Haarnoja et al., "Soft actor-critic: Off-policy maximum entropy deep reinforcement learning with a stochastic actor," International Conference on Machine Learning (ICML), 2018.

27. Q. Yang, G. Wang, A. Sadeghi, G.B. Giannakis, J. Sun, "Two-timescale voltage control in distribution grids using deep reinforcement learning," IEEE Trans. Smart Grid, vol. 11, no. 3, pp. 2313–2323, 2020.

28. E. Foruzan, L.K. Soh, S. Asgarpoor, "Reinforcement learning approach for optimal distributed energy management in a microgrid," IEEE Trans. Power Systems, vol. 33, no. 5, pp. 5749–5758, 2018.

29. Z. Yan, Y. Xu, "A multi-agent deep reinforcement learning method for cooperative load frequency control of a multi-area power system," IEEE Trans. Power Systems, vol. 35, no. 6, pp. 4599–4608, 2020.

30. K. Glory Prasanth, &A.Venmani. (2026). Nonlinear Inference Procedures for Location-Scale Families in Ordered Sequential Reliability Structure. *Results in Nonlinear Analysis*, *9*(2), 14–36.